Random Vibration of Steel Catenary Riser Conveying Fluid Under Wave Excitation

Zhang Wenshou *, *Cai Ruijiao*, *Yang Zhixun*

State Key Laboratory of Structural Analysis for Industrial Equipment, Department of Engineering Mechanics, Dalian University of Technology, Dalian 116024, P. R. China

(Received 10 December 2017; revised 15 January 2018; accepted 20 January 2018)

Abstract: This paper presents a frequency domain approach for the calculation of the random response of fluid-conveying steel catenary risers under random wave force. The partial differential equations of motion of the steel catenary riser under a combination of internal flow and random wave excitation are established based on a series of earlier publications. The mass matrix, stiffness matrix, damping matrix and wave loading for steel catenary riser are derived in frequency domain by using Hamilton's principle. Analysis of free vibrations is then carried out to investigate the effect of flow velocity on natural frequency. By further introducing the pseudo-excitation method, the dynamic analysis of the steel catenary riser subject to wave excitation is performed in frequency domain to see how the flow velocity affects the bending moment response of the steel catenary riser. The parametric studies on the example steel catenary riser show that flow velocity may decrease the natural frequencies and increase the dynamic response of the steel catenary riser. Moreover, the dynamic stability of fluid-conveying steel catenary risers is investigated and the critical fluid velocity is identified.

Key words: dynamic stability; steel catenary riser; dynamic response; internal flow; critical fluid velocity; frequency domain

CLC number: TE3 **Document code**: A **Article ID**: 1005-1120(2018)05-0883-07

0 Introduction

Steel catenary riser (SCR) has been widely used in offshore oil and gas field development because of their cost efficiency and structural simplicity[1]. Dynamic response of fluid-conveying SCR under potential cyclic loading such as the motions of floating support facility and waves is very important in SCR design to ensure safe operation. Besides this, the fluid flowing inside the riser may exert important influence on the overall dynamical behavior[2-3].

The dynamic behavior of pipes conveying fluid has been studied by many researchers[4]. Chucheepsakul et al. proposed the large strain formulations of marine riser from the theoretical point of view[5]. Kaewunruen et al. applied the finite element method to study the nonlinear free vibrations of marine risers[6]. The nonlinear natural frequencies and corresponding mode shapes were determined and the influence of the marine riser's parameters on its nonlinear phenomena was investigated. The study found that the internal flows of the riser reduced the degree of hardening and turned the vibration type from hardening to softening one. Chatjigeorgiou formulated the nonlinear dynamic problem of catenary risers conveying fluid using the Newtonian derivation procedure and potential theory[7]. The effect of the inner flow to the global dynamics of the riser is assessed in both time and frequency domain. Athisakul et al. developed a variational model formulation for static and dynamic analysis of three-dimensional extensible marine riser transporting fluid[8]. They studied the effects of axial extensibility and internal flow on dynamic proper-

* Corresponding author, E-mail address: wszhang@dlut.edu.cn.

How to cite this article: Zhang Wenshou, Cai Ruijiao, Yang Zhixun. Random vibration of steel catenary riser conveying fluid under wave excitation[J]. Trans. Nanjing Univ. Aero. Astro., 2018,35(5):883-889.
http://dx.doi.org/10.16356/j.1005-1120.2018.05.883

ties of three-dimensional marine risers. Meng and Chen formulated nonlinear models of steel catenary risers based on the large strain theory[9]. The parametric studies were carried out to examine the effect of internal fluid velocities and top tension on the nonlinear dynamics of riser undergoing vortex-induced vibration. They found that the internal flows reduced the natural frequencies and the stability of the riser.

This paper aims to develop a method to study the dynamics of SCR conveying fluids under wave excitation. The mass matrix, stiffness matrix, damping matrix and wave force vector of the curved pipe are derived in frequency domain. The wave response of the SCR is computed using the pseudo-excitation method. An extensive parametric study is then carried out to investigate whether any possibly undesirable phenomena occur in transverse vibration of the SCRs caused by fluid flow.

1 Formulation

1.1 Modeling of the system

The system of SCR is formulated under the following assumptions: (1) The SCR can move only in the plane of the figure (i.e. in the in-line direction) and the lateral deflection is considered to be small; (2) The flow inside the SCR is assumed to be a plug flow with constant velocity; (3) The centerline of the SCR is inextensible; (4) The radius of curvature is assumed to be very large compared with the pipe radius, and hence the effects of secondary flow are neglected. The model is shown in Fig. 1. If the displacement is measured from the position of static equilibrium configuration, the governing equations of the SCR under wave excitation can be established based on the Misra's work[10]

$$EI\left(\frac{\partial^4 w}{\partial s^4}+\frac{1}{R_0}\frac{\partial^3 u}{\partial s^3}\right)-\frac{\partial}{\partial s}\left[T\left(\frac{\partial w}{\partial s}+\frac{u}{R_0}\right)\right]+ m_f U^2\left(\frac{\partial^2 w}{\partial s^2}+\frac{1}{R_0}\frac{\partial u}{\partial s}\right)+2m_f U\left(\frac{\partial^2 w}{\partial s\partial t}+\frac{1}{R_0}\frac{\partial u}{\partial t}\right)+ c_r\frac{\partial w}{\partial t}+(m_r+m_f)\frac{\partial^2 w}{\partial t^2}-F_n=0 \tag{1}$$

$$-\frac{EI}{R_0}\left(\frac{\partial^3 w}{\partial s^3}+\frac{1}{R_0}\frac{\partial^2 u}{\partial s^2}\right)-\frac{T}{R_0}\left(\frac{\partial w}{\partial s}+\frac{u}{R_0}\right)- \frac{m_f U^2}{R_0}\left(\frac{\partial w}{\partial s}+\frac{u}{R_0}\right)+m_f U\left(\frac{\partial^2 u}{\partial s\partial t}-\frac{1}{R_0}\frac{\partial w}{\partial t}\right)+ c_r\frac{\partial u}{\partial t}+(m_r+m_f)\frac{\partial^2 u}{\partial t^2}-F_\tau=0 \tag{2}$$

where s is the curvilinear coordinate along the deformed centerline; u and w are the longitudinal and transverse displacements of the SCR, respectively; EI is the flexural stiffness; m_r and m_f are the mass of the SCR per unit length and the mass of fluid per unit length, respectively; c_r is the damping coefficient of the SCR; U is the flow velocity; R_0 is the radius of curvature of the SCR; F_n and F_τ are the external wave force in the normal and tangential directions, respectively; T is the axial tension.

Compared with the Misra's work[10], three major differences should be emphasized: (1) The first difference is that the governing equations in the Misra's work include both dynamic and static parts, and in this study the governing equations include only dynamic part since the static part is determined in advance by solving a two-point boundary value problem. This makes the governing equations simplified. (2) The second difference is that no external excitation existed in the Misra's work so they could eliminate the unknowns by differentiating equations with respect to s. Nevertheless, because of the existence of wave force in this study, differentiating equations with respect to s can cause the inaccuracy in wave force and should be avoided. (3) The last difference is that the element stiffness matrix in Misra's work is non-symmetric. To overcome

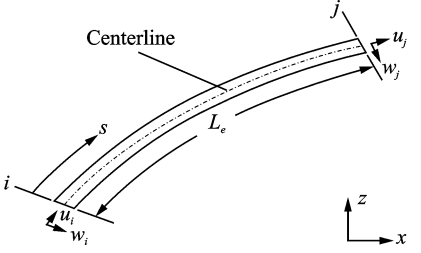

Fig. 1 Curved pipe element with nodes i and j at its extermities

this problem, a new derivation for element stiffness matrix is given in this study and a symmetric element stiffness matrix is obtained.

For a smooth SCR, the wave force in the tangential direction can be neglected, and hence only the wave force in the normal direction on the SCR is considered. The wave force F_n can be expressed by linearized Morison's equation[11]

$$F_n = \frac{1}{2}\rho D C_D A_\sigma \left(v_n - \frac{\partial w}{\partial t}\right) + C_M \frac{\pi}{4}\rho D^2 \frac{\partial v_n}{\partial t} - (C_M - 1)\frac{\pi}{4}\rho D^2 \frac{\partial^2 w}{\partial t^2} \tag{3}$$

where

$$v = \omega \frac{\cosh kz}{\sin h kd}\eta,\ \omega^2 = g\kappa \cdot \tan h \kappa d \tag{4a}$$

$$v_n = v\sin\theta,\ A_\sigma = \sqrt{\frac{8}{\pi}}\sigma_{v_n} \tag{4b}$$

in which z is the vertical location above the bottom of the sea, θ is angle between x-axis and tangent to the centerline of the SCR, ρ is the sea water density, D is the diameter of the SCR, C_D is the drag coefficient, C_M is the inertia coefficient, d is water depth, κ is the wave number, ω is the angular frequency of the wave, v is the horizontal instantaneous flow velocity, v_n is the instantaneous flow velocity component normal to the centerline of the SCR, η is the free surface of the wave with the wave spectrum $S_{\eta\eta}(\omega)$, and σ_{v_n} is the standard deviation (SD) of the velocity.

Substituting Eqs. (3), (4) into Eq. (1), one obtains

$$EI\left(\frac{\partial^4 w}{\partial s^4} + \frac{1}{R_0}\frac{\partial^3 u}{\partial s^3}\right) - \frac{\partial}{\partial s}\left[T\left(\frac{\partial w}{\partial s} + \frac{u}{R_0}\right)\right] + m_f U^2\left(\frac{\partial^2 w}{\partial s^2} + \frac{1}{R_0}\frac{\partial u}{\partial s}\right) + 2m_f U\left(\frac{\partial^2 w}{\partial s \partial t} + \frac{1}{R_0}\frac{\partial u}{\partial t}\right) + c\frac{\partial w}{\partial t} + m\frac{\partial^2 w}{\partial t^2} = \omega \frac{\cosh kz}{\sin h kd}\sin\theta(\varphi_D A_\sigma \eta + \varphi_M \dot{\eta}) \tag{5}$$

where $m = m_r + m_f + \pi(C_M - 1)\rho D^2/4$ is the total mass per unit length of the system, and $c = c_r + \varphi_D A_\sigma$ is the total damping per unit length of the system. While $\varphi_D = C_D \rho D/2$ and $\varphi_M = \pi C_M \rho D^2/4$ are two constants representing the hydrodynamic damping force and inertia force coefficient, respectively.

1.2 Curved pipe element

Using Hamilton's principle, a curved pipe element as shown in Fig. 1 can be derived from the partial differential Eqs. (2), (5). By taking the product of the Eqs. (2), (5) with the arbitrary variational displacement and integrating over the length of the element, one obtains

$$\sum_j \int_0^{L_j} [\delta u L_u(u, w) + \delta w L_w(u, w)] \mathrm{d}s = \sum_j \int_0^{L_j} \delta w R_w \mathrm{d}s \tag{6}$$

where $L_u(u, w)$ represents the left-hand side of Eq. (2); $L_w(u, w)$ and R_w represent the left-hand side and right-hand side of Eq. (5), respectively; L_j is the length of the jth element.

Using the relation

$$\boldsymbol{q}_j(s, t) = \boldsymbol{N}(s)\boldsymbol{q}_j^e(t) \tag{7}$$

where

$$\boldsymbol{q}_j(s, t) = \begin{Bmatrix} u_j(s, t) \\ w_j(s, t) \end{Bmatrix} \tag{8}$$

$$\boldsymbol{N}(s) = \begin{bmatrix} \boldsymbol{N}_u \\ \boldsymbol{N}_w \end{bmatrix} = \begin{bmatrix} N_1 & 0 & 0 & N_4 & 0 & 0 \\ 0 & N_2 & N_3 & 0 & N_5 & N_6 \end{bmatrix} \tag{9}$$

$$\boldsymbol{q}_j^e(t) = [u_i \quad w_i \quad w_i' \quad u_j \quad w_j \quad w_j']^{\mathrm{T}} \tag{10}$$

where the prime represents the derivative with respect to s, and $N_i (i = 1, 2, \cdots, 6)$ represent the shape functions given by

$$N_1 = 1 - s/L_j,\ N_2 = 1 - 3s^2/L_j^2 + 2s^3/L_j^3 \tag{11a}$$

$$N_3 = s(1 - 2s/L_j + s^2/L_j^2),\ N_4 = s/L_j \tag{11b}$$

$$N_5 = 3s^2/L_j^2 - 2s^3/L_j^3,\ N_6 = s(s^2/L_j^2 - s/L_j) \tag{11c}$$

The element mass, damping, stiffness matrix and element force vector are obtained based on Eq. (6)

$$\boldsymbol{M}^e = m\int_0^{L_e} \boldsymbol{N}_w^{\mathrm{T}}\boldsymbol{N}_w \mathrm{d}s + (m_r + m_f)\int_0^{L_e} \boldsymbol{N}_u^{\mathrm{T}}\boldsymbol{N}_u \mathrm{d}s \tag{12a}$$

$$\boldsymbol{C}^e = c\int_0^{L_e} \boldsymbol{N}_w^{\mathrm{T}}\boldsymbol{N}_w \mathrm{d}s + c_r\int_0^{L_e} \boldsymbol{N}_u^{\mathrm{T}}\boldsymbol{N}_u \mathrm{d}s + 2m_f U\int_0^{L_e} (\boldsymbol{N}_w^{\mathrm{T}}\boldsymbol{N}_w' + \boldsymbol{N}_u^{\mathrm{T}}\boldsymbol{N}_u'/2)\,\mathrm{d}s + (2m_f U/R_0)\int_0^{L_e} (\boldsymbol{N}_w^{\mathrm{T}}\boldsymbol{N}_u - \boldsymbol{N}_u^{\mathrm{T}}\boldsymbol{N}_w/2)\,\mathrm{d}s \tag{12b}$$

$$\boldsymbol{K}^e = EI\int_0^{L_e} \boldsymbol{N}_w''^{\mathrm{T}}\boldsymbol{N}_w'' \mathrm{d}s + (EI/R_0^2)\int_0^{L_e} \boldsymbol{N}_u'^{\mathrm{T}}N_u' \mathrm{d}s + (EI/R_0)\int_0^{L_e} (\boldsymbol{N}_w''^{\mathrm{T}}\boldsymbol{N}_u' + \boldsymbol{N}'^{\mathrm{T}}_u\boldsymbol{N}_w'')\,\mathrm{d}s + \int_0^{L_e} (T - m_f U^2)\,\boldsymbol{N}_w'^{\mathrm{T}}\boldsymbol{N}_w' \mathrm{d}s +$$

$$(1/R_0)\int_0^{L_e}(T-m_fU^2)\,(\boldsymbol{N}_w'^{\mathrm{T}}\boldsymbol{N}_u+\boldsymbol{N}_u^{\mathrm{T}}\boldsymbol{N}_w')\,\mathrm{d}s+$$

$$(1/R_0^2)\int_0^{L_e}(T-m_fU^2)\,\boldsymbol{N}_u^{\mathrm{T}}\boldsymbol{N}_u\mathrm{d}s \tag{12c}$$

$$\boldsymbol{F}^e=\int_0^{L_e}\boldsymbol{N}_w^{\mathrm{T}}\omega\,\frac{\cosh kz}{\sinh kd}\sin\theta(\varphi_D A_\sigma\eta+\varphi_M\dot{\eta})\mathrm{d}s=$$

$$\boldsymbol{\alpha}^e\eta+\boldsymbol{\beta}^e\dot{\eta} \tag{13}$$

where L_e is the length of the element under consideration, and

$$\boldsymbol{\alpha}^e=\varphi_D\omega\int_0^{L_e}\boldsymbol{N}_w^{\mathrm{T}}A_\sigma\,\frac{\cosh kz}{\sinh kd}\sin\theta\mathrm{d}s \tag{14a}$$

$$\boldsymbol{\beta}^e=\varphi_M\omega\int_0^{L_e}\boldsymbol{N}_w^{\mathrm{T}}\,\frac{\cosh kz}{\sinh kd}\sin\theta\mathrm{d}s \tag{14b}$$

By considering the centerline of the SCR to be inextensible, the element stiffness matrix can be modified by setting

$$\boldsymbol{K}_{11}^e=\boldsymbol{K}_{44}^e=\mu,\ \boldsymbol{K}_{14}^e=\boldsymbol{K}_{41}^e=-\mu \tag{15}$$

where μ is a large positive number.

2 Solution

By using the curved pipe element, the SCR is discretized into n elements with varying curvature from element to element. The global mass matrix $\boldsymbol{M}$, global damping matrix $\boldsymbol{C}$, global stiffness matrix $\boldsymbol{K}$, global nodal force vector $\boldsymbol{F}$ and global nodal displacement vector $\boldsymbol{q}$ are assembled in the usual finite element manner from individual element contributions. The partial differential Eqs. (2), (5) can then be expressed as the ordinary differential equations

$$\boldsymbol{M}\ddot{\boldsymbol{q}}(t)+\boldsymbol{C}\dot{\boldsymbol{q}}(t)+\boldsymbol{K}\boldsymbol{q}(t)=\boldsymbol{\alpha}\eta(t)+\boldsymbol{\beta}\dot{\eta}(t) \tag{16}$$

According to the pseudo-excitation method, the free surface wave elevation $\eta(t)$ can be constituted as[12]

$$\eta(t)=\sqrt{S_{\eta\eta}(\omega)}\,\mathrm{e}^{\mathrm{i}\omega t} \tag{17}$$

Substituting Eq. (17) into Eq. (16), one obtains

$$\boldsymbol{M}\ddot{\boldsymbol{q}}(t)+\boldsymbol{C}\dot{\boldsymbol{q}}(t)+\boldsymbol{K}\boldsymbol{q}(t)=(\boldsymbol{\alpha}+\mathrm{i}\omega\boldsymbol{\beta})\,\sqrt{S_{\eta\eta}(\omega)}\,\mathrm{e}^{\mathrm{i}\omega t} \tag{18}$$

Using the first r normal modes for mode superposition, i. e.

$$\boldsymbol{q}(t)=\sum_{j=1}^{r}p_j(t)\phi_j=\boldsymbol{\Phi}\boldsymbol{p}(t) \tag{19}$$

where $\boldsymbol{\Phi}=[\phi_1\quad\phi_2\quad\cdots\quad\phi_r]$ is the modal matrix, and $\boldsymbol{p}(t)=[p_1(t)\quad p_2(t)\quad\cdots\quad p_r(t)]^{\mathrm{T}}$ is the generalized coordinate vector. Then Eq. (18) becomes

$$\bar{\boldsymbol{M}}\ddot{\boldsymbol{p}}(t)+\bar{\boldsymbol{C}}\dot{\boldsymbol{p}}(t)+\bar{\boldsymbol{K}}\boldsymbol{p}(t)=(\bar{\alpha}+\mathrm{i}\omega\bar{\boldsymbol{\beta}})\,\sqrt{S_{\eta\eta}(\omega)}\,\mathrm{e}^{\mathrm{i}\omega t} \tag{20}$$

where

$$\bar{\boldsymbol{M}}=\boldsymbol{\Phi}^{\mathrm{T}}\boldsymbol{M}\boldsymbol{\Phi},\ \bar{\boldsymbol{C}}=\boldsymbol{\Phi}^{\mathrm{T}}\boldsymbol{C}\boldsymbol{\Phi},\ \bar{\boldsymbol{K}}=\boldsymbol{\Phi}^{\mathrm{T}}\boldsymbol{K}\boldsymbol{\Phi} \tag{21a}$$

$$\bar{\boldsymbol{\alpha}}=\boldsymbol{\Phi}^{\mathrm{T}}\boldsymbol{\alpha},\ \bar{\boldsymbol{\beta}}=\boldsymbol{\Phi}^{\mathrm{T}}\boldsymbol{\beta} \tag{21b}$$

The particular solution of Eq. (20) is

$$\boldsymbol{p}(t)=(\bar{\boldsymbol{K}}-\omega^2\bar{\boldsymbol{M}}+\mathrm{i}\omega\bar{\boldsymbol{C}})^{-1}(\bar{\boldsymbol{\alpha}}+\mathrm{i}\omega\bar{\boldsymbol{\beta}})\,\sqrt{S_{\eta\eta}(\omega)}\,\mathrm{e}^{\mathrm{i}\omega t} \tag{22}$$

Substituting Eq. (22) into Eq. (19) gives the pseudo-displacement as

$$\boldsymbol{q}(t)=\boldsymbol{\Phi}(\bar{\boldsymbol{K}}-\omega^2\bar{\boldsymbol{M}}+\mathrm{i}\omega\bar{\boldsymbol{C}})^{-1}(\bar{\boldsymbol{\alpha}}+\mathrm{i}\omega\bar{\boldsymbol{\beta}})\,\sqrt{S_{\eta\eta}(\omega)}\,\mathrm{e}^{\mathrm{i}\omega t} \tag{23}$$

Denoting the jth component of $\boldsymbol{q}(t)$ as q_j, the response spectral density of q_j is given by

$$\boldsymbol{S}_{q_jq_j}(\omega)=q_j^*q_j \tag{24}$$

where the superscript $*$ represents complex conjugate. The SD of q_j can be expressed as

$$\sigma_{q_j}=\left[\int_0^{\infty}S_{q_jq_j}(\omega)\mathrm{d}\omega\right]^{1/2} \tag{25}$$

3 Numerical Results

A SCR conveying petroleum is selected as an example for parametric study and application. The SCR is attached to a semi-submersible located in 1 250 m of water, as shown in Fig. 2. The main parameters used in the case study are given in Table 1. The irregular waves are characterized by a JONSWAP (Joint North Sea Wave Project) spectrum defined as[13]

$$S_{\eta\eta}(\omega)=487(1-0.287\ln\gamma)H_s^2T_p^{-4}\omega^{-5}\cdot$$

$$\exp(-1\,948T_p^{-4}\omega^{-4})\gamma^{\exp\left[-\frac{(0.159\omega T_p-1)^2}{2\sigma^2}\right]} \tag{26}$$

where γ, σ_a and σ_b are the shape parameters and their mean values are $\gamma=3.3$, $\sigma=\begin{cases}0.07 & \omega\leqslant 2\pi/T_p\\ 0.09 & \omega>2\pi/T_p\end{cases}$; H_s is the significant wave height; and T_p is the peak period.

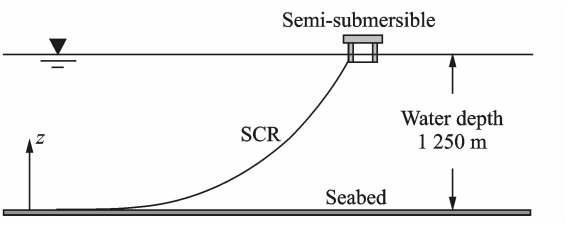

Fig. 2 Schematic of an example SCR

Table 1 Main parameters used in case study

Parameter	Value
Water depth / m	1 250
Outside diameter / m	0.324
Density of SCR / (kg • m^{-3})	7 850
Damping coefficient / (Ns • m^{-2})	0.009 2
Drag coefficient	0.8
Significant wave height / m	8.7
Density of petroleum /(kg • m^{-3})	860
Density of sea water / (kg • m^{-3})	1 025
Inside diameter / m	0.222
Elastic modulus / (N • m^{-2})	2.06×10^{11}
Hang-off angle / (°)	10
Inertia coefficient	2.0
Peak period / s	12.3

For the deepwater SCR, Duan et al. Use the following equations for determining the configuration and tension due to its submerged weight[14]

$$EI\frac{d^3\theta}{ds^3}-T\frac{d\theta}{ds}+(m_r+m_f)g\cos\theta=0 \quad (27)$$

$$\frac{dT}{ds}=(m_r+m_f)g\sin\theta \quad (28)$$

Eqs. (27),(28) are two-point boundary value problems which can be solved by the function BVP4C in MATLAB.

The effects of the heave motion of the semi-submersible on the configuration and tension of SCR can be evaluated by means of investigating the influence of water depth. Fig. 3 shows the configuration of the SCR with different water depths. It is seen that the configurations of SCR for water depths of 1 240, 1 250 and 1 260 m coincide with each other well. Therefore, the configurations of the SCR are not sensitive to heave motion of the semi-submersible. The same conclusion can also be reached for the tensions of SCR for water depths of 1 240,1 250 and 1 260 m, as shown in Fig. 4. Hence, the configuration and tension of SCR for the water depth of 1 250 m are used in this study.

Fig. 5 displays variations of the first five natural frequencies of SCR with flow velocity within the range between 0 and 200 m/s. Clearly, the natural frequencies always decrease with the increasing of the flow velocity, and eventually the natural frequencies tend to be diminished to zero. The fact that the natural frequencies monotonically decrease with the increasing flow velocity means that the SCR becomes softer when the flow velocity increases. When the flow velocity is below 100 m/s, the modal frequencies are not sensitive to the flow velocity. As the flow velocity becomes larger and larger, the natural frequencies decrease rapidly. The first natural frequency vanishes when the flow velocity reaches its critical value of about 160 m/s. As a result, the SCR loses stability in its first mode. Similar phenomena were also observed by Misra et al. who investigated a clamped-clamped semi-circular pipe conveying fluid[10].

Fig. 6 shows the variation of the SD of bending moment at the touchdown point (TDP) of

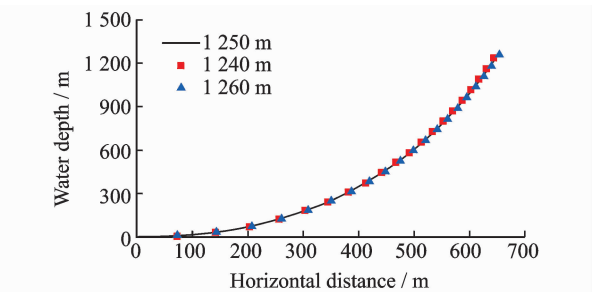

Fig. 3 Configuration of SCR with different water depths

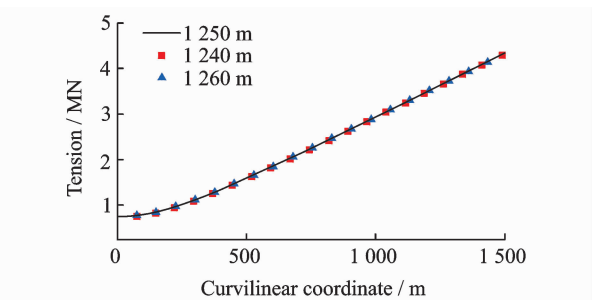

Fig. 4 Tension of SCR with different water depths

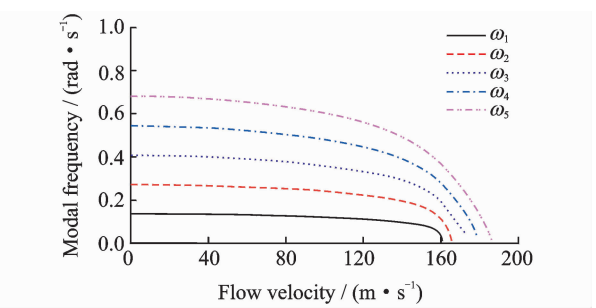

Fig. 5 Variations of natural frequencies with flow velocity

SCR with flow velocity within the range between 0 and 160 m/s. It is seen that there are a number of sharp peaks, which correspond to natural frequencies of SCR and represent resonance responses. As the flow velocity increases, the number of peaks becomes closely spaced. This is because the resonance frequencies change from lower modes to higher modes which are closely spaced. It is also seen that the bending moment response increases slightly when the flow velocity becomes larger. This is consistent with the results from free vibration analysis in Fig. 5.

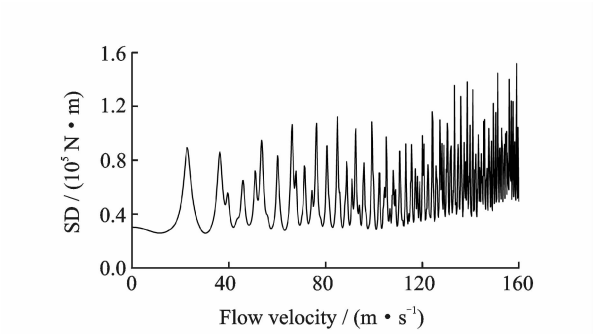

Fig. 6 Variation of SD of bending moment at TDP

Fig. 7 shows the variations of the SD of bending moment along the SCR at the flow velocities of 0 and 60 m/s. It is seen that the magnitude of bending moment response depends on the value of flow velocity. The larger flow velocity leads to larger bending moment response. This may be because of the decrease in stiffness of SCR due to flow velocity. It is also seen that the bending moment responses achieve the maximum values at the TDP of SCR and sharply decrease in the zone away from the TDP. Thus, TDP is the critical location for SCR design.

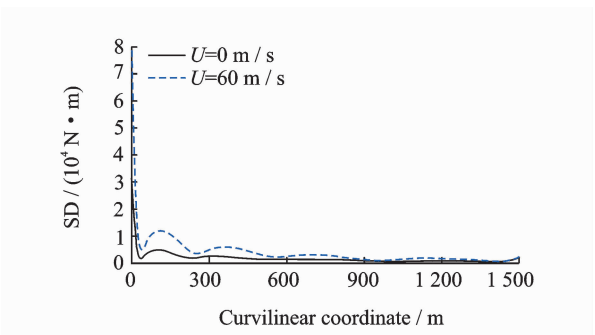

Fig. 7 Variations of SD of bending moment along SCR with different flow velocities

4 Conclusions

A frequency domain approach for the analysis of SCR conveying fluid under wave excitation is proposed. The equations of SCR conveying fluid under wave excitation are established. The stiffness, mass and damping matrices are derived using Hamilton's principle. Parametric studies are then carried out to investigate the effect of flow velocity on the dynamic response of SCR, and some conclusions can be drawn as follows:

(1) Flow velocity monotonically decreases the natural frequencies of SCR, namely, the stiffness of SCR. For a given SCR, there exists a critical value of flow velocity by which the SCR loses stability.

(2) The magnitude of bending moment response depends on the value of flow velocity. If the flow velocity is beyond the critical value, the bending moment response tends to infinity.

(3) The maximum value of bending moment response of SCR under wave excitation is located at the TDP of SCR. It sharply decreases in the zone away from the TDP.

Acknowledgement

This work was supported by the National Natural Science Foundation of China (No. 11372060).

References:

[1] MEKHA B, BHAT S. Newer frontiers in the design of steel catenary risers for floating production systems[C]//International Conference on Ocean, Offshore and Arctic Engineering. Nantes: American Society of Mechanical Engineers, 2013: OMAE2013-11562.

[2] IBRAHIM R A. Overview of mechanics of pipes conveying fluids-Part I: Fundamental studies[J]. Journal of Pressure Vessel Technology, 2010, 132(3): 034001-32.

[3] IBRAHIM R A. Mechanics of pipes conveying fluids-Part II: Applications and fluid elastic problems[J]. Journal of Pressure Vessel Technology, 2011, 133(2): 024001-30.

[4] PAÏDOUSSIS M P, Li G X. Pipes conveying fluid: A model dynamical problem[J]. Journal of Fluids and Structures, 1993, 7(2): 137-204.

[5] CHUCHEEPSAKUL S, MONPRAPUSSORN T,

HUANG T. Large strain formulations of extensible flexible marine pipes transporting fluid[J]. Journal of Fluids and Structures, 2003,17(2):185-224.

[6] KAEWUNRUEN S, CHIRAVATCHRADEJ J, CHUCHEEPSAKUL S. Nonlinear free vibrations of marine risers/pipes transporting fluid[J]. Ocean Engineering, 2005,32(3/4):417-440.

[7] CHATJIGEORGIOU I K. On the effect of internal flow on vibrating catenary risers in three dimensions [J]. Engineering Structures, 2010, 32(10): 3313-3329.

[8] ATHISAKUL C, MONPRAPUSSORN T, CHUCHEEPSAKUL S. A variational formulation for three-dimensional analysis of extensible marine riser transporting fluid [J]. Ocean Engineering, 2011,38(4):609-620.

[9] MENG D, CHEN L. Nonlinear free vibrations and vortex-induced vibrations of fluid-conveying steel catenary riser[J]. Applied Ocean Research, 2012, 34 (1):52-67.

[10] MISRA A K, PAÏDOUSSIS M P, VAN K S. On the dynamics of curved pipes transporting fluid. Part I: Inextensible theory[J]. Journal of Fluids and Structures, 1988,2(3):221-244.

[11] BORGMAN L E. Ocean wave simulation for engineering design[J]. Proceedings of ASCE Journal of Waterways and Harbors Divisions, 1969, 95:557-583.

[12] LIN J H, ZHANG W S, LI J J. Structural responses to arbitrarily coherent stationary random excitations [J]. Computers & Structures, 1994, 50(5):629-633.

[13] HASSELMANN K, BARNETT T P, BOUWS E, et al. Measurements of wind-wave growth and swell decay during the Joint North Sea Wave Project (JONSWAP)[J]. Deutsche Hydrographische Zeitschrift, 1973,12(2):1-95.

[14] DUAN M, CHEN J, TIAN K, et al. A mechanical model for deepwater steel catenary riser transfer process during installation [J]. Proceedings of the Institution of Mechanical Engineers Part M: Journal of Engineering for the Maritime Environment, 2013, 227(1):3-11.

Prof. **Zhang Wenshou** received the B. S. and M. S. degrees in engineering mechanics from Dalian University of Technology, Dalian, China, in 1983 and 1986, respectively. In 2000, he received his Ph. D. degree in civil engineering from the Hong Kong Polytechnic University. From 2001 to present, he has been a full professor in Dalian University of Technology. His research has focused on vibration control, fluid-structure interaction, vibration of bridges and buildings.

Ms. **Cai Ruijiao** received the B. S. degree in theoretical and applied mechanics from Shenyang University of Chemical Technology, Shenyang, China, in 2014 and M. S. degree in engineering mechanics from Dalian University of Technology, Dalian, China, in 2017. Her research is focused on fluid-structure interaction.

Dr. **Yang Zhixun** received the M. S. degree in engineering mechanics from Dalian University of Technology, Dalian, China, in 2012. From 2013 to present, he has been a Ph. D. candidate in Dalian University of Technology. His research is focused on ocean engineering.

(Production Editor: Sun Jing)